Springer Series in
Surface Sciences
11

J. F. van der Veen
M. A. Van Hove (Eds.)

The Structure of Surfaces II

Proceedings of the 2nd International Conference on the Structure of Surfaces (ICSOS II), Amsterdam, The Netherlands, June 22–25, 1987

With 343 Figures

Springer-Verlag Berlin Heidelberg New York
London Paris Tokyo

Editor: Gerhard Ertl

Structure and Phase Transitions of Incommensurate Xe Layers on Pt(111)

K. Kern, P. Zeppenfeld, R. David, and G. Comsa

Institut für Grenzflächenforschung und Vakuumphysik,
KFA Jülich, Postfach 1913, D-5170 Jülich, Fed. Rep. of Germany

Considerable theoretical and experimental attention has been paid in the last decade to the investigation of critical phenomena in systems of reduced dimensionality (1D or 2D). Since the pioneering work of Peirls and Landau in the 30's it has been realized that the physical properties of two dimensional (2D) matter are fascinating and differ substantially from those of bulk matter. A widespread possibility to realize 2D-systems is to adsorb atoms or molecules onto a solid surface. This particular way of producing quasi two dimensional systems gives rise to a new class of phase transitions in the adsorbed layer; the registry-disregistry transitions, also named commensurate-incommensurate transitions.

In fig.1 we show an example for a commensurate adlayer structure, the $(\sqrt{3}\times\sqrt{3})R30°$ phase of Xe on the Pt(111) surface. On fcc(111) faces the Xe atoms (probably) prefer to sit in three fold hollow sites. These preferred adsorption sites form a triangular lattice. As a consequence of their size, the Xe atoms can only occupy second neighbor lattice sites (rather than nearest neighbor sites) resulting in a commensurate structure whose lattice parameter is only expanded by 9% with respect to the natural 2D Xe-lattice parameter. The maximum coverage in this $(\sqrt{3}\times\sqrt{3})R30°$ commensurate structure is obviously $\Theta_{Xe}=1/3$ ($\Theta_{Xe}=1$ corresponds to 1.5×10^{15} atoms/cm^2, the density of Pt atoms in the (111) plane). Only one third of the adsorption sites are occupied, i.e.

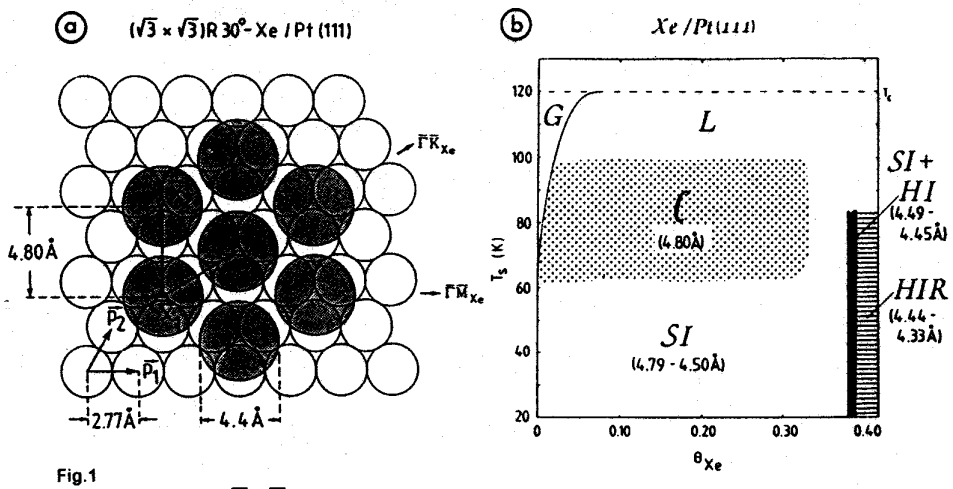

Fig.1
a)Commensurate $(\sqrt{3}\times\sqrt{3})R30°$ Xe monolayer adsorbed on Pt(111); b) schematic phase diagram of Xe monolayers on Pt(111)

there exist three energetically degenerate commensurate sublattices. The commensurate Xe-lattice being expanded, the coverage can be increased beyond $\Theta_{Xe}=1/3$. However, above this limit it is no longer possible for all adatoms to occupy preferred adsorption sites, and the adlayer becomes incommensurate, eventually approaching a lattice parameter characteristic of bulk Xe.

How can an incommensurate adlayer on a crystal surface best be described? Far from commensurability the incommensurate monolayer can be regarded as a triangular lattice with spacing corresponding to coverage. Due to the slight variation of the adsorption energy within the substrate unit cell (see fig.3), this lattice is weakly modulated. Novaco and McTague /1/ have used this idea of weakly modulated 2D-solids and found that the energy of these monolayers is dependent on the orientation relative to the substrate, and in particular that the orientation which minimizes the total energy is expected to deviate from the high symmetry directions of the substrate. The resulting orientation of the adlayer is a consequence of the fact that in a 2D Lennard Jones solid the transverse phonon modes are much softer than the longitudinal modes, thus favoring a transverse displacive movement of the atoms. Novaco-McTague type rotations have been observed in numerous incommensurate adlayers /2/.

Near commensurability, however, an incommensurate monolayer is commonly thought to be built up of large commensurate regions separated by incommensurate domain walls, such that the distance between domain walls is large compared to the width of the walls. This approach is based on the ideas of Frank and van der Merwe /3/ and has been developed in great detail in the 70's by several theoreticians /4/. On hexagonal substrates the domain walls may run along any of the three degenerate high symmetry directions. The actual realization of one or another domain wall network depends on the wall crossing energy Λ: for attractive wall crossings ($\Lambda<0$) a hexagonal network of domain walls (HI) is predicted, while for repulsive walls ($\Lambda>0$) a striped network of domain walls (SI) should appear. The Bak-Mukamel-Villain-Wentowska (BMVW) theory further predicts that the C → HI transition should be first order while the C → SI transition should be second order /5/. At higher incommensurabilities, the SI-phase is expected to transform to a HI-phase by a first order transition /6/, before finally rotating out of the high symmetry direction of the substrate (HIR).

Until recently, there was only scarce experimental evidence for these stringent theoretical predictions. The most intensively studied experimental system, Kr on Graphite, shows a continuous transition, although hexagonal symmetry is preserved. It is Xe on Pt(111) which appears to be the first adsorption system fully consistent with the BMVW-theory /5/. We have investigated this 2D-system in great detail by means of high resolution helium scattering. The inferred schematic phase diagram in the coverage-temperature plane is shown in fig.1b. This phase diagram has been obtained by measuring the $(2,2)_{Xe}$ and $(1,2)_{Xe}$ diffraction patterns. As shown in detail in ref.2 and 7 this analysis allows a unique determination of the symmetry, orientation and lattice parameter of the various solid Xe phases.

The $(\sqrt{3}\times\sqrt{3})R30°$ commensurate phase (C) has been found to be stable in an extended temperature (62K-99K) and coverage range (0.02-0.33) /8/. At completion the C-phase consists of coherent domains which are about 800Å in diameter, as deduced from the measured He-diffraction peak widths. As the coverage is increased above $\Theta_{Xe}>0.33$ the Xe-layer undergoes a commensurate-incommensurate transition. He-diffraction spectra measured in the incommensurate region for coverages less than 0.38 always reveal the following spot patterns. The measured (2,2) spot consists of an out of plane doublet located at $Q^{2,2}_{comm}+\varepsilon/2$, symmetrical

with respect to the $\overline{\Gamma M}_{x_s}$-direction, and a single peak located in the $\overline{\Gamma M}_{x_s}$-azimuth at $Q^{1,2}_{comm} + 2\varepsilon$. The (1,2) spot exhibits a peak at the commensurate position $Q^{1,2}_{comm}$ in the $\overline{\Gamma K}_{x_s}$-azimuth and a weak out of plane doublet at $Q^{1,2}_{comm} + (3/4)\varepsilon\sqrt{3}$. These observed diffraction patterns are characteristic for a striped incommensurate phase (SI) with the uniaxial compression in the $\overline{\Gamma M}_{x_s}$-direction, and with the domain walls strongly relaxed /7/. Close to the CI-transition, however, for misfits less than about 3%, we observe an additional on axis satellite peak at $Q^{1,2}_{comm} + \varepsilon/2$ in the (2,2) diffraction patterns. Detailed studies of the structure factor for the different domain wall types as a function of the wall relaxation have shown that this additional satellite is consistent with the occurrence of superheavy striped domain walls almost 5-6 atoms wide /9/. Thus, the domain walls in the striped incommensurate phase of Xe/Pt(111) exhibit a strong relaxation tendency. This trend is consistent with the wall relaxations observed for Kr on graphite. Total energy calculations /10/, molecular dynamics calculations /11/ as well as analysis of synchrotron X-ray scattering data /12/ reveal a wall relaxation of four to six atoms.

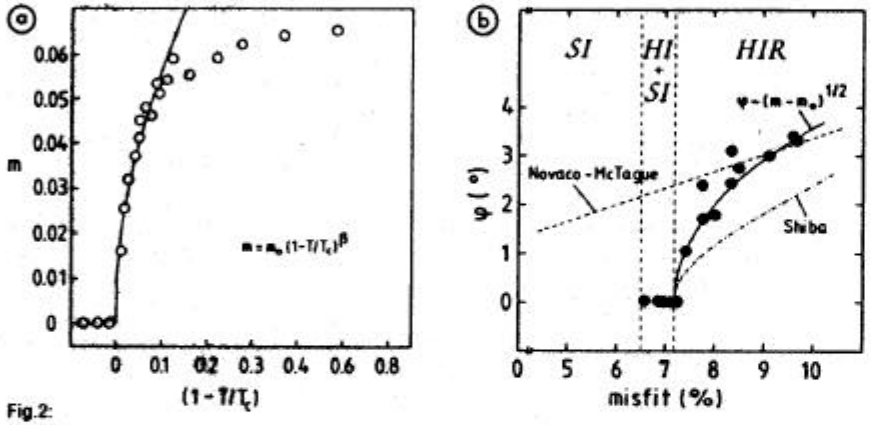

Fig.2:
a) $\overline{\Gamma M}$-uniaxial misfit m vs reduced temperature during the C-SI transition. The solid line represents the power law fit. b) Rotation angle φ of Xe monolayers on Pt(111) vs misfit m

The C-SI transition is the simplest realization of a domain wall driven phase transition in two dimensions, in that the domain walls form a one dimensional array of discommensurations. This allows the application of an exactly solvable 1D-soliton model. In their pioneering work Frank and van der Merwe /3/ solved this model for T=0K, i.e. neglecting thermal fluctuations, with a continuum mean field ansatz. Pokrovsky and Talapov (PT) /13/ have included these fluctuation effects; for $T \neq 0K$ the domain walls can meander and collide, giving rise to an entropy mediated repulsive force between meandering walls of the form $F \sim T^2/l^2$, where l is the distance between nearest neighbor walls. Because of this inverse square behavior, the inverse wall separation, i.e. the misfit m, in the weakly incommensurate phase should follow a power law of the form:

$$m = \frac{1}{l} \sim (1 - \frac{T}{T_c})^{1/2} \qquad [1]$$

In fig.2a we have analyzed the data of the C-SI transition in the weakly incommensurate phase with a least-squares fit of a power law form $m = m_0(1 - T/T_c)^{\beta}$; the best fit parameters are $T_c = 61.7K$, $m_0 = 0.18$ and $\beta = 0.51 \pm 0.04$. The value of β is in good agreement with the Pokrovsky-

Talapov prediction. Data points have only be included in the fit up to misfits of about 4%. The cutoff at ~ 4% has been chosen in accordance with Erbil et al. /14/, who have found the $\beta = 1/2$ power law to be valid in this range for bromine intercalated graphite. For larger values, the misfit variation with reduced temperature is roughly linear. In this region the distance between walls is of order of the wall width and the PT-theory is not applicable (for a detailed discussion, see below).

When increasing the coverage above ~ 0.38 an additional on axis peak at $Q^{1,2}_{comm} + \sqrt{3}\,\varepsilon$ appeared in the (1,2) diffraction spots. This marks the transition from the SI-phase to the nonrotated hexagonal incommensurate HI-phase /2/. Diffraction patterns composed of a peak at $Q^{1,2}_{comm}$ and a doublet at $Q^{1,2}_{comm} + (3/4)\sqrt{3}\,\varepsilon$ originating from a SI-phase, and an on axis peak at $Q^{1,2}_{comm} + \sqrt{3}\,\varepsilon$ originating from a HI-phase are observed in the coverage range $0.38 \leq \Theta_{x_s} \leq 0.39$, with the $Q^{1,2}_{comm} + \sqrt{3}\,\varepsilon$ peak intensity progressively increasing with coverage. Thus, we conclude that the SI-phase transforms at a critical coverage of about 0.38 to a HI-phase in a first order transition.

Finally, when increasing the coverage above 0.39 only the peaks characterizing the hexagonal phase are observed (the SI-phase disappears). However, these peaks at $Q^{1,2}_{comm} + \sqrt{3}\,\varepsilon$ and $Q^{1,2}_{comm} + 2\varepsilon$ (in the (1,2) and (2,2) diffraction patterns, respectively) start to split azimuthally with increasing coverage. This obviously characterizes a Novaco-McTague rotated phase. In fig.2b we show the variation of the rotation angle φ with average misfit m during the *HI* → *HIR* transition. The experimental data are compared with theoretical calculations of Novaco and McTague (NM) /1/ and of Shiba /15/. The dashed line is the NM-linear response theory for a Cauchy solid. Although this model describes the measured rotation angle at large misfits quite well, it fails at the HI-HIR transition region, particularly it does not predict the finite misfit for the onset of rotation. As shown by Villain /16/ this failure is preordained in the NM-theory, because the assumptions made are not expected to be valid for small incommensurabilities. Shiba, on the other hand, predicted a continuous HI-HIR transition to occur at some finite misfit, which was correlated to the crossover from the domain wall regime at small incommensurabilities to the modulation regime at large incommensurabilities. His curve for a Cauchy solid is drawn in fig.4 as dashed-dotted line for the value of his parameter l_0 (= 10) which sets the critical misfit, at which the HI-HIR transition occurs, to 7.2% as observed experimentally. Shiba's domain wall corrections only give a qualitative account of the overall variation of rotation angle versus misfit. A quantitative agreement with the data is obtained by a power law of the form $\varphi \sim (m - m_0)^{1/2}$ with $m_0 = 0.072$, shown as solid line in fig.2b. It is worth noting that a similar power law behavior has been observed for the rotation angle in Cs-intercalated graphite /17/ and in Kr layers on the basal plane of graphite /18/.

The richness of the phase diagram of Xe monolayers on such a "smooth" surface like the (111) face of platinum is rather surprising. The various solid phases (C,SI,HI,HIR) of noble gas adlayers on crystal surfaces and their mutual transitions arise as a result of competing interactions: lateral adatom versus adatom-substrate interaction. It is in particular the delicate force balance between the lateral adatom potential and the lateral modulation of the substrate holding potential (i.e. the variation of the adsorption energy within the substrate unit cell, e.g. hollow, bridge, on top site). It is a widespread belief that the variation of the modulation of this potential (periodic corrugation) for noble gases on close packed metal surfaces is negligible. In several experiments Webb and coworkers /19/ were able to show that the properties of adsorbed monolayers of Xe,Kr and Ar on Ag(111) to a good approximation can be described by assuming a laterally flat holding potential. However, the occurrence of pronounced registry effects in Xe monolayers on the close packed Pt(111) surface sheds a new light on the question of the lateral potential modulations of smooth metal surfaces. In a recent investigation Black and Bopp /20/ studied the Xe/Pt(111) system by molecular dynamics techniques. They demonstrated that, if one assumes that the corrugation of

the holding potential is of the order of 3meV or less, even the existence of the commensurate $\sqrt{3}$ structure is not reproducible; the Xe layer, in order to be commensurate, has to be expanded with respect to its "natural" lattice by about 9%, and the shallow corrugation does not withstand this strain.

In order to facilitate realistic estimates for the corrugation amplitude of the Xe/Pt(111) holding potential we have performed thermodynamic adsorption measurements /21/. In fig.3a we show the measured isosteric heat of adsorption q_{st} as a function of Θ_{Xe}. The heat of adsorption increases steadily from 277meV at zero coverage to about 312 meV at $\Theta_{Xe} = 0.33$ (indicating attractive lateral interactions). Upon further increase of the Xe-coverage, i.e. at the CI transition, a substantial drop in q_{st} to a value of about 280 meV is observed. This drop of q_{st} reflects the binding energy difference between Xe adsorption energy at three fold hollow sites in the commensurate phase and the average energy of the various sites occupied by the Xe-atoms in the incommensurate phase. Thus the value $\Delta q_{st} = q_{st}^c - q_{st}' \simeq 30meV$ provides a lower bound for the surface diffusional barrier of Xe on Pt(111). This value is supported by recent photoemission and mobility measurements /21/. A similar value, 50meV, has been measured for Xe on W(110) - also a rather closed packed surface - by the field emission current flucutuation method /22/.

The knowledge of the diffusional barrier allows the construction of a realistic Xe-Pt(111) potential. It has been shown by Steele /23/, that the physisorption potential of rare gas atoms on a crystal surface, to a good approximation, is reproduced by a Fourier expansion cut off after the first order term. Owing to the rapid convergence of the Fourier series, the second order term is already 2 orders of magnitude smaller than the first order term, and for a fcc(111) surface we obtain:

$$V(\vec{r}) = V_0(z) + V_G(z)\ \{\cos(2\pi s_1) + \cos(2\pi s_2) + \cos(2\pi s_1 + 2\pi s_2)\} \qquad [2]$$

where $V_0(z)$ is the mean potential energy of an adatom at a distance z from the substrate surface, V_G is the principle Fourier amplitude and s_1 and s_2 are the coordinates of the atoms in the substrate surface unit cell. At low temperatures $V_0(z)$ can be replaced by its harmonic approximation:

$$V_0(z) \simeq V_0 + \frac{1}{2} V_0''(z - z_0)^2 \qquad [3]$$

Since $V_T - V_H = 4.5V_G$ and $V_B - V_H = 4V_G$ in a two dimensional model (here V_T, V_B and V_H are the potentials at on top, bridge and hollow sites, respectively) we can construct the Xe-Pt(111) potential shown in fig.3b using the following parameters: V_0 = 277meV (ref.24), V_0'' = 342meV (ref.25), V_g = 7.5meV and z_0 = 3.10Å (ref.20).

Also shown in fig.3b is the Xe-Pt(111) potential used by Black and Bopp /20/. Besides the overall height of the potential corrugation the main difference between the two potentials is the magnitude of the diffusion barrier of the bridge position. Whereas in the Fourier potential the diffusional barrier of bridge and on top position is nearly equal, in the potential used by Black and Bopp the barrier of the bridge site is almost a factor of 7 smaller than the barrier of on top positions. Obviously, this low bridge barrier hardly hinders the free migration of Xe atoms at temperatures greater than 60K, where the commensurate phase is actually observed and this phase cannot be stabilized in the calculations.

We close the paper with a discussion of the incommensurate phase of Xe monolayers on Pt(111). Beyond the completion of the $(\sqrt{3} \times \sqrt{3})R30°$ commensurate phase, a continuous phase transition to a striped incommensurate phase (SI), with superheavy domain walls running in the

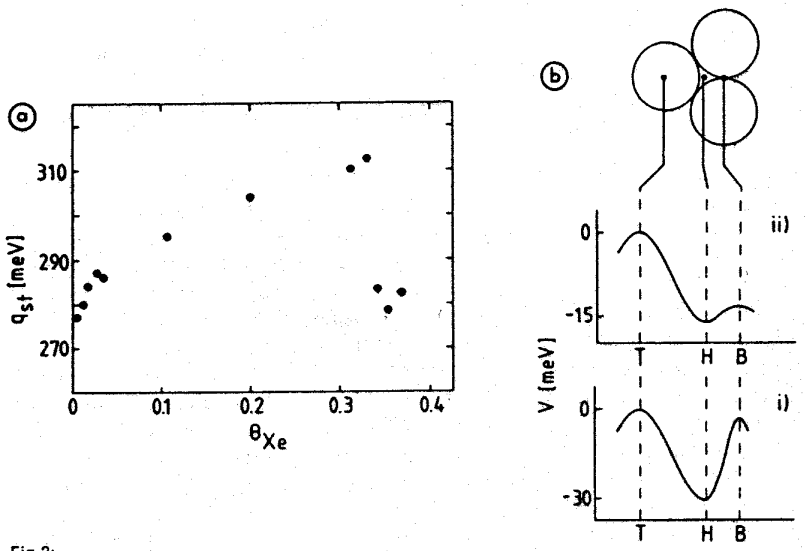

Fig.3:
a)Isosteric heat of adsorption q_{st} of Xe on Pt(111) as a function of coverage Θ_{Xe}. b) The lateral Xe-Pt surface potential modulation i) for the Fourier ansatz with the parameters listed in the text ii) for the potential used by Black and Bopp /20/

$\overline{\Gamma K}_{Xe}$ -direction, occurs. In contrast to the CI-transition of Kr on graphite, which is in fact a melting transition due to the instability of the hexagonal weakly incommensurate phase with respect to the formation of free dislocations (reentrant melting), the C-SI transition of Xe/Pt(111) is a solid-solid transition with the incommensurability simply related to the domain wall density. According to Coppersmith et al. /6/ striped structures are stable if the number of sublattices, p (here, 3), is larger than $\sqrt{8}$, whereas for hexagonal structures the criterion is $p > 7.5 \pm 1.5$. The incommensurability in the weakly incommensurate phase follows a $\beta = 0.51 \pm 0.04$ power law versus reduced temperature. This exponent is in good agreement with the $\beta = 1/2$ prediction of Pokrovsky and Talapov. The Pokrovsky-Talapov model may essentially be applied to a substrate of uniaxial symmetry, although the original model calculations are performed for an isotropic substrate, and thus should be applicable to the isotropic Pt(111) substrate. However, in a recent study, Haldane and Villain /26/ pointed out that in the case of rare gas monolayers on *metal* surfaces, substrate induced electric dipole interactions might be responsible for the square root law. Moreover, they demonstrated that even in the case of an insulating substrate (no induced dipole forces) the Pokrovsky-Talapov square root behavior should be valid only for very small misfits ($m \leq 0.001$!). It is difficult to distinguish at the present stage definitely between the thermal fluctuation mechanism of Pokrovsky and Talapov or the substrate induced dipole mechanism of Haldane and Villain. However, it is worth noting that the experimental range of validity of the square root law in 2D-striped domain wall phases has been found to be much larger (a factor of $\simeq$30) than the limit given by Haldane and Villain, for "insulating" substrates (Br intercalated graphite /14/) as well as for metal substrates (Xe/Cu(110) /27/, Xe/Pt(111) /7/).

The width of the superheavy domain walls in the striped phase, as obtained from an analysis of the satellite peak intensities, amounts to about 6 row spacings (FWHM). With increasing

incommensurability the total length of the domain walls increases, while the wall thickness is expected to remain constant /11/, giving rise to smaller and more numerous commensurate domains. For misfits larger than 3-4%, i.e. where the interwall distance is only three times the width of the walls, in the diffraction patterns the striped incommensurate layer can no longer be distinguished from an uniaxially compressed layer.

The most direct implication of the existence of a striped phase in Xe layers on Pt(111) is that the wall crossing energy is significantly positive. This is at variance with the observations made for Kr layers on graphite, where the crossing energy was always found to be negative or at least only slightly positive (so that the entropy gain due to the free breathing of the honeycomb lattice is sufficient to stabilize the hexagonal symmetry). Gooding et al. /10/ have studied the influence of the substrate potential modulation on the different wall energies .They found that for large potential modulations striped arrays of discommensurations might have lowest energy. This goes along with the large potential modulation observed for the Xe/Pt(111) system. The extended misfit range ($0 < m \leq 7.2\%$) in which the striped structure appears to be stable, is somewhat puzzling in view of the recent results by Halpin-Healy and Kardar /28/. They have studied the occurrence of striped structures in the "striped helical Potts lattice gas model". Their results reveal a strong correlation between the width of the striped phase regime and the wall thickness. Striped structures in an extended coverage range should appear only for "sharp" domain walls: with increasing wall thickness this range is expected to shrink substantially. The energy cost due to the wall repulsion seems to be too large for thick walls. They conclude that the wall width of 4-5 in Kr monolayers on graphite might be responsible for the absence of a striped phase in this system. The wall width in Xe layers on Pt(111) is even larger: the size of coverage range in which the striped phase is stable corresponds in Halpin-Healy and Kardar's calculations to wall widths of 1-2.

At misfits of about 6.5% the striped phase transforms to a hexagonal incommensurate R30° phase (HI) by a first order transition. This transition occurs at a coverage where the domain wall separation is about twice the domain wall width. The HI-phase, in which the monolayer recovers its hexagonal *R30°* symmetry, is stable only in a small coverage range, before, upon further compression, it displays a continuous transition from the *R30°* to a rotated orientation (HIR). The onset of rotation occurs at a critical misfit of 7.2% and the rotation angle follows a power-law form with the mean field exponent $\beta = 1/2$.

Xe on Pt(111) appears to be the first 2D system fully consistent with the BMVW-theory, i.e. is the first system displaying the full sequence of $C \rightarrow SI \rightarrow HI \rightarrow HIR$ transitions with increasing incommensurability. This theory is a mean field theory, neglecting thermal fluctuations. However, Halpin-Healy and Kardar /29/ have studied recently the various domain wall phases in the framework of a generalized helical Potts model, including finite temperature effects and two species of domain walls. Their results were in general agreement with the T=0K BMVW-theory; in particular they pointed out that the $C \rightarrow SI \rightarrow HI$ sequence only occurs when assuming repulsive heavy and superheavy wall crossings.

References

1. A.D.Novaco and J.P.McTague: Phys.Rev. B19,5299(1979)
2. K.Kern: Phys.Rev. B35,8265(1987), and references therein
3. F.C.Frank and J.H.van der Merwe: Proc.Roy.Soc.London A198,205(1949)
4. J.Villain and M.B.Gordon: Surf.Sci. 125,1(1983), and references therein
5. P.Bak, D.Mukamel, J.Villain, and K.Wentowska: Phys.Rev. B19,1610(1979)
6. S.N.Coppersmith, D.S.Fisher, B.I.Halperin, P.A.Lee, and W.F.Brinkman: Phys.Rev. B25,349(1982)
7. K.Kern, R.David, P.Zeppenfeld, R.L.Palmer, and G.Comsa: Solid State Comm. 62,391(1987)
8. K.Kern, R.David, R.L.Palmer, and G.Comsa: Phys.Rev.Lett 56,620(1986)
9. P.Zeppenfeld, K.Kern, and G.Comsa: to be published
10. R.J.Gooding, B.Joos, and B.Bergersen: Phys.Rev. B27,7669(1983)
11. F.F.Abraham, W.E.Rudge, D.J.Auerbach, and S.W.Koch: Phys.Rev.Lett. 52,445(1984)
12. P.W.Stephens, P.A.Heiney, R.J.Birgeneau, P.M.Horn, D.E.Moncton, and G.S.Brown: Phys.Rev. B29,3512(1987)
13. V.L.Pokrovsky and T.L.Talapov: Sov.Phys.JETP 51,134(1980)
14. A.Erbil, A.R.Kortan, R.J.Biregeneau, and M.S.Dresselhaus: Phys.Rev. B28,6329(1983)
15. H.Shiba: J.Phys.Soc.Jpn. 48,211(1980)
16. J.Villain: Phys.Rev.Lett. 42,36(1978)
17. R.Clarke, N.Caswell, and P.M.Horn: Phys.Rev.Lett. 43,2018(1979)
18. K.L.D'Amico, D.E.Moncton, E.D.Specht, R.J.Birgeneau, S.E.Nagler, and P.M.Horn: Phys.Rev.Lett. 53,2250(1984)
19. J.Unguris, L.W.Bruch, E.R.Moog, and M.B.Webb: Surf.Sci. 109,522(1981), and references therein
20. J.Black and B.Bopp: Phys.Rev. B34,7410(1986)
21. K.Kern, P.Zeppenfeld, R.David, and G.Comsa: submitted to Surf.Sci.
22. J.R.Chen and R.Gomer: Surf.Sci. 94,456(1980)
23. W.A.Steele: Surf.Sci. 36,317(1973)
24. K.Kern, R.David, R.L.Palmer, and G.Comsa: Surf.Sci: 175,L669(1986)
25. K.Kern, R.David, R.L.Palmer, and G.Comsa: Phys.Rev.Lett. 56,2823(1986)
26. F.D.M.Haldane and J.Villain: J.Physique (Paris) 42,1673(1981)
27. M.Jaubert, M.Glachant, M.Bienfait, and G.Boato: Phys.Rev.Lett. 46,1679(1981)
28. T.Halpin-Healy and M.Kardar: Phys.Rev. B34,318(1986)
29. T.Halpin-Healy and M.Kardar: Phys.Rev. B31,1664(1985)